

# The rare extended radio-loud narrow-line Seyfert 1 galaxy SDSS J1030+5516 at high resolution

K. É. Gabányi<sup>1</sup> • S. Frey • P. Veres • A. Moór

**Abstract** Recently, Rakshit et al. (2018) reported the discovery of SDSS J103024.95+551622.7, a radio-loud narrow-line Seyfert 1 galaxy having a  $\sim 100$  kpc scale double-lobed radio structure. Here we analyse archival radio interferometric imaging data taken with the Very Large Array (VLA) at 5 GHz, and with the Very Long Baseline Array (VLBA) at 4.3 and 7.6 GHz. Two hotspots and a compact core are detected with the VLA at arcsec scale, while a single milliarcsec-scale compact radio core is seen with the highest resolution VLBA observations. The *Fermi* Large Area Telescope did not detect  $\gamma$ -ray emission at the position of this source. In the mid-infrared, the *Wide-field Infrared Survey Explorer* satellite light curve, covering more than 7 years and including the most recent data points, hints on flux density variability at  $3.4 \mu\text{m}$ . Our findings support the notion that this source is a young version of Fanaroff–Riley type II radio galaxies.

**Keywords** galaxies: active; galaxies: Seyfert; galaxies: individual: SDSS J103024.95+551622.7

K. É. Gabányi

MTA-ELTE Extragalactic Astrophysics Research Group,  
krisztina.g@gmail.com

S. Frey

Konkoly Observatory, MTA Research Centre for Astronomy and  
Earth Sciences

P. Veres

Center for Space Plasma and Aeronomic Research, University of  
Alabama in Huntsville

A. Moór

Konkoly Observatory, MTA Research Centre for Astronomy and  
Earth Sciences

<sup>1</sup>Konkoly Observatory, MTA Research Centre for Astronomy and  
Earth Sciences

## 1 Introduction

Narrow-line Seyfert 1 galaxies (NLS1) form a peculiar subclass of active galactic nuclei (AGN). They are defined by their narrow permitted optical lines (the full width at half maximum, FWHM, of  $\text{H}\beta$  line is below  $2000 \text{ km s}^{-1}$ , Goodrich 1989), a flux ratio of  $[\text{O III}]\lambda 5007$  to  $\text{H}\beta$  smaller than 3 (Osterbrock and Pogge 1985), and the strong emission of the Fe II multiplets. However, Cracco et al. (2016) showed that having strong iron lines may not be a distinctive property of NLS1 sources in accordance with the study of quasar emission lines of Boroson and Green (1992), which showed the anticorrelation between the strength of Fe II and O III lines.

The narrow permitted lines of NLS1 sources are explained with their relatively lower-mass central black holes,  $10^6 - 10^8 M_{\odot}$  (Mathur 2000), which consequently means high accretion rates close to the Eddington limit (Boroson and Green 1992). Based upon these, Mathur (2000) proposed that NLS1 sources can be young AGN residing in rejuvenated galaxies. Alternatively, the narrow  $\text{H}\beta$  lines of NLS1 sources can be due to orientation effect, if their disk-like broad-line regions are seen pole-on (Decarli et al. 2008).

Similarly to AGN in general, a small fraction,  $\sim 7\%$  of NLS1 sources are radio-loud (Komossa et al. 2006; Zhou et al. 2006), where radio-loudness is determined by the ratio of the 6 cm radio to the  $4400 \text{ \AA}$  optical flux density following Kellermann et al. (1989). Singh and Chand (2018) studied the radio properties of a large sample of optically-selected NLS1 sources, and found that the radio-detected ones have small sizes,  $< 30$  kpc. The most radio-loud NLS1 sources (and the ones with the highest radio luminosity investigated by Singh and Chand 2018) show blazar-like properties: flat radio spectrum, compact radio cores, high brightness temperatures, significant variability, flat X-ray spectra,

and altogether blazar-like spectral energy distribution (SED; e.g. Yuan et al. 2008). Several of them were also detected in  $\gamma$ -rays with the *Fermi* satellite (for a full list, see Romano et al. 2018), and in a few of them superluminally moving radio jet components were imaged with very long baseline interferometry (VLBI) technique (Lister et al. 2016). Therefore these sources, similarly to blazars, are thought to possess relativistic radio jets inclined at small angle to the line of sight.

Few of the radio-loud NLS1 sources have kpc-scale (from a few tens of kpc to  $\sim 100$  kpc) radio structures. Doi et al. (2012) found that the detection rate of extended radio emission in NLS1 sources is lower than in broad-line AGN. This is confirmed more recently by Berton et al. (2018). They observed 74 NLS1 sources and found that the majority of flat-spectrum radio-loud NLS1 sources have compact morphology on kpc scale. In most of the extended radio-loud NLS1 sources, the radio emission is two-sided (Doi et al. 2012; Richards and Lister 2015; Congiu et al. 2017; Gabányi et al. 2018b).

Recently, Rakshit et al. (2018) reported the discovery of a radio-loud NLS1 source, SDSS J103024.95+551622.7 (hereafter J1030+5516) with arcsec-scale structure similar to those of Fanaroff–Riley type II radio galaxies (FR II, Fanaroff and Riley 1974). The projected linear size,  $\sim 110$  kpc is among the largest values in radio-loud NLS1 sources. Using low-resolution ( $\sim 5''$ ) radio data of J1030+5516 from the Faint Images of the Radio Sky at Twenty-Centimeters (FIRST) survey (Becker et al. 1995), Rakshit et al. (2018) argue that the inclination angle of the jet in the core region is  $< 12^\circ$  with respect to the line of sight.

Here we present sub-arcsec resolution archival Very Large Array (VLA) A-configuration data, and milli-arcsec (mas) resolution VLBI data of J1030+5516, which support the claims of Rakshit et al. (2018). Additionally, we analysed more than 10 yr of *Fermi* Large Area Telescope (LAT; Acero et al. 2015, and references therein) data to constrain the high-energy properties of the source. We also re-evaluated the mid-infrared light curves covering more than 7 yr, obtained with the *Wide-field Infrared Survey Explorer* (*WISE*, Wright et al. 2010) satellite.

In the following, we assume a flat  $\Lambda$ CDM cosmological model with  $H_0 = 70 \text{ km s}^{-1} \text{ Mpc}^{-1}$  and  $\Omega_m = 0.27$ . At the redshift of J1030+5516,  $z = 0.435$ ,  $1''$  angular size corresponds to a projected linear size of 5.65 kpc.

## 2 Observing data

### 2.1 Archival VLA radio data

J1030+5516 was observed at 5 GHz with the VLA in its most extended A configuration on 1992 October 20 (project code: AF233). The raw data were obtained from the US National Radio Astronomy Observatory (NRAO) archive<sup>1</sup>. The on-source integration time was 1 min, the total bandwidth was 100 MHz. Phases and amplitudes were calibrated in the NRAO Astronomical Image Processing System (AIPS, Greisen 2003) in a standard way. The flux density scale was set using the amplitude calibrator source 3C286. We used the DIFMAP (Shepherd et al. 1994) software for imaging and for fitting Gaussian brightness distribution model components directly to the interferometer visibility data.

### 2.2 Archival VLBA radio data

J1030+5516 was observed with the Very Long Baseline Array (VLBA) on 2016 May 28 at 4.3 and 7.6 GHz (project code: BP192, PI: L. Petrov) in the framework of the wide-field VLBA calibrator survey (L. Petrov 2019, in preparation). Nine (Brewster, Fort Davis, Hancock, Kitt Peak, Los Alamos, North Liberty, Owens Valley, Pie Town, St. Croix) and eight (all the above but Hancock) antennas of the array were used at the lower and higher frequency, respectively. The bandwidth was 256 MHz and the integration time was nearly 1 min at both frequencies. The calibrated visibilities were obtained from the Astrotego website<sup>2</sup>.

### 2.3 Archival *Fermi*/LAT $\gamma$ -ray data

We analysed the archival *Fermi*/LAT data of J1030+5516. We looked for  $\gamma$ -ray signals in the available 10.3-year data which cover the time range between 2008 August 4 and 2018 November 26. We derived *Fermi*/LAT upper limits using the routines included in the `fermipy` package (Wood et al. 2017). We selected a  $15^\circ$  circular region around the position of J1030+5516, and an energy range of 0.1 – 100 GeV. We used Pass 8, SOURCE type photons, with *P8R2\_SOURCE\_V6* responses. The fit included a diffuse galactic foreground (`gll_iem_v6`) and an isotropic component (`iso_P8R2_SOURCE_V6_v06`).

<sup>1</sup><https://archive.nrao.edu/>

<sup>2</sup>[http://astrotego.org/vlbi\\_images](http://astrotego.org/vlbi_images), maintained by L. Petrov

## 2.4 WISE data

The mid-infrared *WISE* satellite scanned the whole sky in four bands at 3.4, 4.6, 12, and  $22\mu\text{m}$  (referred as W1, W2, W3, and W4) during its original mission phase in 2010 (Wright et al. 2010). Afterwards, the satellite measurements are continued within the framework of the NEOWISE (Near-Earth Object WISE) project (Mainzer et al. 2014). After four months of NEOWISE observations, the satellite was hibernated for 34 months. Then the NEOWISE Reactivation Mission continued. In this currently on-going phase, observations are conducted only at the two shorter wavelength bands, since the cooling material required for W3 and W4 receivers has been depleted. The *WISE* satellite observes the same regions of the sky in every  $\sim 180$  days.

We downloaded the *WISE* single exposure data<sup>3</sup> up until 2017 November, and followed the procedure as in Gabányi et al. (2018a). We adapted the guidelines in the Explanatory Supplement Series<sup>4</sup> to discard bad quality data points. None of the measurements were affected by the South-Atlantic Anomaly, or scattered light from the Moon. We used only those measurements for which the frame image quality score (`‘qi_fact’`) was 1.0, since values less than 1.0 mark data where residual light system motion may degrade the flux measurements. Ten per cent of data were discarded because of this effect. The contamination and confusion flags (`‘cc_flags’`) did not indicate problems for any of the measurements.

The final light curve contains 177 points grouped into ten mission phases both in W1 and W2 bands. Each mission phase lasted usually for  $\lesssim 2$  days and contains 12 – 16 points, except for one mission phase, which is the combination of two  $\sim 1$ -day long observations separated by 2 days and contains 26 data points.

## 3 Results

### 3.1 VLA data

The 5-GHz VLA-A observation revealed three distinct features, the core, the southwest (SW) and the northeast (NE) lobes (Fig. 1). This structure is in good agreement with the lower-resolution FIRST image presented by Rakshit et al. (2018). Three circular Gaussian model components can adequately describe the radio structure. Their parameters are given in Table 1. The distance between the components fitted to

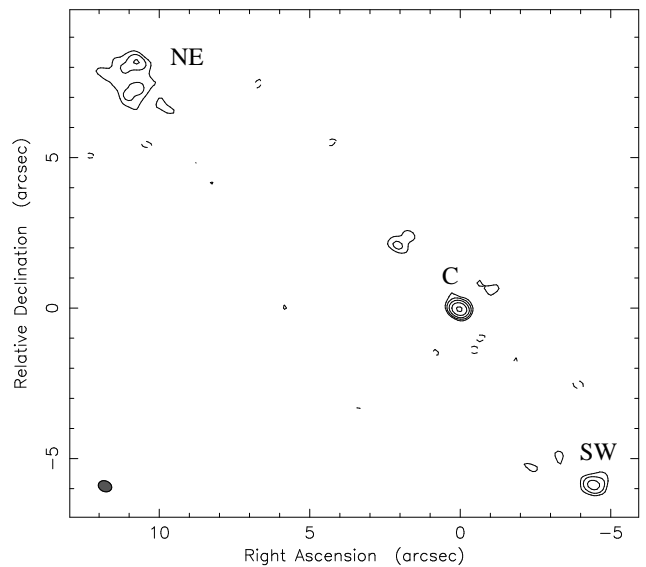


**Fig. 1** 5-GHz VLA image of J1030+5516 taken on 1992 October 20. The image is centred at the brightest pixel at right ascension  $10^{\text{h}}30^{\text{m}}24^{\text{s}}.947$  and declination  $55^{\circ}16'22''.6$ . Peak brightness is  $8.4 \text{ mJy beam}^{-1}$ , the lowest contours are drawn at  $\pm 0.5 \text{ mJy beam}^{-1}$ , corresponding to  $\sim 3\sigma$  image noise level. (Dashed lines represent negative contours.) The positive contours increase by a factor of 2. The restoring beam is  $0''.5 \times 0''.4$  (FWHM) with a major axis position angle  $68^{\circ}$ , as shown in the lower left corner of the image. The three fitted components listed in Table 1 are labeled

the hotspots in the SW and NE lobes is  $20''.43 \pm 0''.01$ , which agrees well with the  $20''.5$  source size at 1.4 GHz, as derived by Rakshit et al. (2018) from the FIRST image.

Using the overall spectral index value  $\alpha = -0.65$  (defined as  $S \propto \nu^{\alpha}$ , where  $S$  is the flux density and  $\nu$  the frequency) and the integrated flux density  $S_{1.4} = 155 \text{ mJy}$  derived from the 1.4-GHz FIRST data by Rakshit et al. (2018), the flux density at 5 GHz can be expected as  $\sim 68 \text{ mJy}$ . The sum of flux densities of the fitted components (Table 1),  $S_5 = 27.8 \text{ mJy}$ , is well below this value, indicating that a significant amount of diffuse radio emission was resolved out in the 5-GHz VLA-A observation.

### 3.2 VLBA data

At both frequencies, a single unresolved component was detected with the VLBA. There was no additional radio-emitting feature down to  $0.8 \text{ mJy beam}^{-1}$  within the undistorted field of view with a radius of  $0''.3$  at 4.3 GHz, and down to  $1.1 \text{ mJy beam}^{-1}$  within the undistorted field of view with a radius of  $0''.2$  at 7.6 GHz.

We used the DIFMAP (Shepherd et al. 1994) software to fit the visibilities with a circular Gaussian brightness distribution. At 4.3 GHz, the radio emission can

<sup>3</sup><http://irsa.ipac.caltech.edu/Missions/wise.html>

<sup>4</sup><http://wise2.ipac.caltech.edu/docs/release/allwise/expsup/sec3.2.html>

**Table 1** Parameters of the circular Gaussian components fitted to the 5-GHz VLA visibilities

ID	Flux density (mJy)	Relative RA (arcsec)	Relative Dec. (arcsec)	FWHM size (mas)
C	$9.3 \pm 0.4$	–	–	$86 \pm 37$
SW	$4.8 \pm 0.6$	$-4.47 \pm 0.03$	$-5.84 \pm 0.03$	$346 \pm 52$
NE	$13.7 \pm 1.7$	$10.87 \pm 0.08$	$7.67 \pm 0.07$	$1386 \pm 140$

Notes: component name in Col. 1, flux density in Col. 2, offset in right ascension and declination with respect to the central component C in Cols. 3 and 4, and the FWHM size in Col. 5

be best described by a point source model. During model-fitting using a Gaussian brightness distribution as a starting model, the FWHM size of the feature converged to an unrealistically small value ( $\sim 10^{-6}$  mas), indicating the unresolved nature of the detected component. The flux density of the point source model component is  $S_{4.3} = 10.6 \pm 0.3$  mJy.

At 7.6 GHz, a stable fit could be reached with using a single circular Gaussian component. Its parameters are: flux density  $S_{7.6} = 15.2 \pm 0.5$  mJy, FWHM diameter  $\theta = 0.31 \pm 0.09$  mas. However, this size is still smaller than the minimum resolvable angular size of the interferometer array, 0.4 mas, calculated following the formula of Kovalev et al. (2005). Therefore J1030+5516 remained unresolved with VLBI at 7.6 GHz as well.

Using the 0.4 mas upper limit to the source size, we can calculate a lower limit to the brightness temperature:

$$T_B = 1.22 \times 10^{12} (1+z) \frac{S}{\theta^2 \nu^2} \text{K}, \quad (1)$$

where  $z$  is the redshift,  $S$  is the flux density in Jy,  $\nu$  is the observing frequency in GHz, and  $\theta$  is the FWHM size of the Gaussian component in mas. Thus, the lower limit to the brightness temperature of J1030+5516 is  $T_B \geq 3 \times 10^9$  K. This value is below the equipartition brightness temperature limit ( $\sim 5 \times 10^{10}$  K; Readhead 1994) by an order of magnitude. However, since it is a lower limit only, it does not exclude the possibility of Doppler boosting caused by relativistic beaming in the jet. More sensitive and higher-resolution VLBI data would be needed to place tighter constraints on the angular size of the compact central source in J1030+5516 and thus on the brightness temperature.

Using these simultaneous dual-frequency VLBA observations, we can derive the two-point spectral index  $\alpha_{4.3}^{7.6} = 0.6 \pm 0.2$  of the core, indicating an inverted radio spectrum of the most compact component. This is not in contrast with the spectral index derived by Rakshit et al. (2018) ( $\alpha = -0.65 \pm 0.04$ ), since that value was obtained using low-resolution radio observations. Those measure the total flux density of J1030+5516 which is dominated by the steep-spectrum lobes and diffuse emission, completely resolved out on the long baselines of the VLBA.

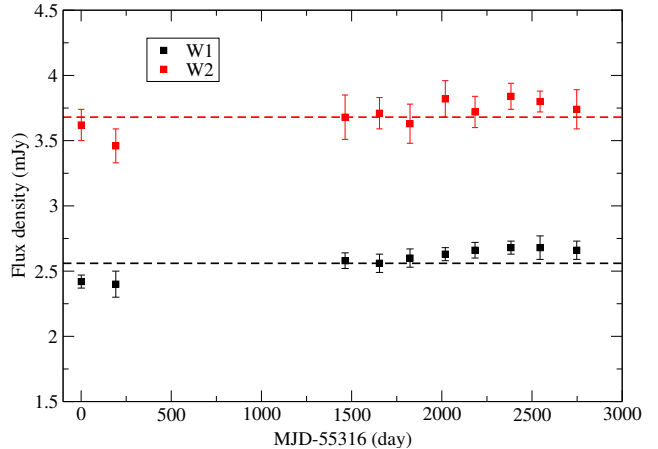


**Fig. 2** Infrared light curves of J1030+5516, measured by the *WISE* satellite. Black and red symbols represent measurements made at  $3.4 \mu\text{m}$  (W1) and  $4.6 \mu\text{m}$  (W2), respectively. The symbols are average values of each mission phase, the error bars represent the variability within each mission phase. The dashed lines show the long-term average flux densities in the two bands

### 3.3 *Fermi*/LAT data

No  $\gamma$ -ray emitting source was detected in the available *Fermi*/LAT data at the position of J1030+5516. The upper limits of the  $\gamma$ -ray fluxes in six energy ranges are given in Table 2.

### 3.4 *WISE* mid-infrared lightcurve

We converted the *WISE* magnitudes to flux densities, following the description in the Explanatory Supple-

**Table 2** *Fermi* upper limits of the  $\gamma$ -ray flux of J1030+5516

Energy range (GeV)	Flux ( $\text{MeV cm}^{-2} \text{s}^{-1}$ )
0.1 – 0.316	$< 4.5 \cdot 10^{-7}$
0.316 – 1	$< 3.9 \cdot 10^{-8}$
1 – 3.162	$< 6.8 \cdot 10^{-8}$
3.162 – 10	$< 2.8 \cdot 10^{-8}$
10 – 31.622	$< 6.6 \cdot 10^{-8}$
31.622 – 100	$< 1.4 \cdot 10^{-7}$

ment Series.<sup>5</sup> To investigate the variability, we calculated the reduced  $\chi^2$  for all the data in a given band, and for each mission phase, separately. For every single mission phase, the reduced  $\chi^2 \lesssim 2$ , indicating no variability on a few-day long time scale. The reduced  $\chi^2$  values for all measurements are 3.3 at  $3.4\mu\text{m}$  and 2.8 at  $4.6\mu\text{m}$ , showing a hint of variability at the shorter wavelength.

Rakshit et al. (2018) also analysed the infrared light curve of J1030+5516 measured with the *WISE* satellite. At the time of their publication only eight mission phases were available, until 2016 November. They found that the object is not variable at  $3.4\mu\text{m}$  and  $4.6\mu\text{m}$ . We also calculated the reduced  $\chi^2$  using the first eight mission phases used by Rakshit et al. (2018). We found that the reduced  $\chi^2$  are lower for both bands, 3.1 at  $3.4\mu\text{m}$  and 2.4 at  $4.6\mu\text{m}$ .

In Fig. 2, we plot the weighted average flux densities and the standard deviations for each mission phase in both bands.

#### 4 Discussion

The obtained lower limit of the brightness temperature of the mas-scale radio emitting core of J1030+5516 agrees well with the values derived by Gu et al. (2015) for a sample of 14 radio-loud NLS1 sources,  $10^{8.4}\text{K} < T_{\text{B}} < 10^{11.4}\text{K}$ . These low values compared to powerful blazar jets are explained by intrinsically low jet power by Gu et al. (2015). The brightness temperature measured in J1030+5516 is also similar to another NLS1 source with a radio structure extended to  $\sim 150\text{kpc}$ , SDSS J110006.07+442144.3 (Gabányi et al. 2018b). Richards and Lister (2015) investigated three radio-loud NLS1 galaxies with kpc-scale radio structures and found mildly relativistic jets. Comparing the mas-scale structures, J1030+5516 is more compact and its brightness temperature is 3 – 20 times larger than the three NLS1 sources studied by Richards and Lister (2015).

The flux density of the core component measured at 5 GHz with the VLA at arcsec scale ( $9.3 \pm 0.4\text{mJy}$ ) is below the value measured at mas-scale resolution with the VLBA at a slightly lower frequency of 4.3 GHz ( $10.6 \pm 0.3\text{mJy}$ ). As this cannot be explained by resolution effect, it is more likely related to variability of the radio flux density.

In the standard picture of expanding radio galaxies, the lobe located closer to the observer is seen farther

away from the host galaxy in projection (Longair and Riley 1979), thus the arm-length ratio of the brighter to the fainter lobe is larger than one. In J1030+5516, the distance between the brighter NE lobe and the central compact radio feature, C is  $d_{\text{NE}} = 13''.3 \pm 0''.1$ , while the fainter SW lobe is at  $d_{\text{SW}} = 7''.35 \pm 0''.04$ . Therefore, it is most likely that the NE feature is at the approaching side of the source.

The arm-length ratio of the approaching to the receding lobes can be used to estimate the inclination angle ( $i$ ) of the source, assuming there is no significant difference in the medium surrounding the jets on the two sides of the host galaxy. Using the equation of Taylor and Vermeulen (1997), the arm-length ratio can be given as

$$\frac{d_{\text{NE}}}{d_{\text{SW}}} = \frac{1 + \beta \cos i}{1 - \beta \cos i} \quad (2)$$

From the VLA data of J1030+5516, the arm-length ratio is 1.81, thus  $\beta \cos i = 0.29$ , which gives a lower limit for the jet speed  $\beta > 0.3$ , and an upper limit for the inclination angle  $i < 73^\circ$ . Similar equation describes the flux density ratio of the jet and counter-jet side (Taylor and Vermeulen 1997):

$$\frac{S_{\text{NE}}}{S_{\text{SW}}} = \left( \frac{1 + \beta \cos i}{1 - \beta \cos i} \right)^{k-\alpha}, \quad (3)$$

where  $k$  equals 2 for continuous jet, and 3 for discrete jet components. Rakshit et al. (2018) using the FIRST data obtained a flux density ratio of 4.35, from which using the spectral index  $\alpha = -0.65$  they derived  $\beta > 0.2$ , and  $i < 79^\circ$ , which agree with our values obtained from the arm-length ratio. The higher resolution 5-GHz VLA data give a flux density ratio of the approaching and receding lobe of  $2.85 \pm 1.8$ , which agrees within the errors with the value Rakshit et al. (2018) used. (Since we have no information on the spectral index of these radio features, we did not use it further to calculate the  $\beta \cos i$  value.)

The Doppler factor is defined as,

$$\delta = \frac{1}{\gamma(1 - \beta \cos i)}, \quad (4)$$

where  $\gamma = 1/\sqrt{1 - \beta^2}$  is the Lorentz factor. Using the value  $\beta \cos i = 0.29$ , and the lower limit on  $\beta$ , 0.29, one can obtain an upper limit on the Doppler factor,  $\delta < 1.34$ .

Doi et al. (2012) estimated the Doppler factor of a few radio-loud NLS1 sources by comparing the observed and intrinsic core powers. Fitting the VLA data we obtained the core flux density at 5 GHz. Assuming the spectral index of the core derived from

<sup>5</sup><http://wise2.ipac.caltech.edu/docs/release/allsky/expsup/sec4.4h.html>

the VLBA data ( $\alpha_{4.3}^{7.6} = 0.6$ ), the observed 5-GHz power of the core is  $3.6 \cdot 10^{24} \text{ W Hz}^{-1}$ . The intrinsic core power can be estimated using the empirical correlation found for radio galaxies,  $\log P_{5\text{GHz}}^{\text{core}} = (0.62 \pm 0.04) \log P_{408\text{MHz}}^{\text{total}} + (7.6 \pm 1.1)$ , where  $P_{408\text{MHz}}^{\text{total}}$  is the source's total power at 408 MHz (Giovannini et al. 2001). The closest frequency where the flux density of J1030+5516 was measured is 365 MHz within the framework of the Texas survey (Douglas et al. 1996). We used that value ( $0.474 \pm 0.038 \text{ Jy}$ ) and the spectral index of the whole source derived by Rakshit et al. (2018) to calculate  $P_{408\text{MHz}}^{\text{total}}$ . The corresponding intrinsic 5-GHz core power is  $\sim 10^{24} \text{ W Hz}^{-1}$ . Following Doi et al. (2012), if the difference between the observed and intrinsic core power is caused by relativistic beaming, their ratio can be given as  $\delta^{3-\alpha}$ . This implies a  $\delta = 1.7$ . However, the uncertainty of the estimation of intrinsic core power allows for lower  $\delta$  values and as high as 12. Rakshit et al. (2018) also used the above argument to estimate a Doppler factor. Instead of the core power, they used the intrinsic and observed core dominance parameter and obtained  $\delta = 3.3$ . The derived  $\delta$  values do not contradict the result of the VLBA observation which gave a lower limit of the brightness temperature. On the other hand,  $\delta > 1.34$  cannot be accommodated with the  $\beta \cos i = 0.29$  derived from the kpc-scale structure. Thus, if we accept the higher Doppler factors derived from the power of the core component, either the jet direction,  $i$ , or the jet speed,  $\beta$ , or both of them change significantly between the kpc and pc scale. The fact that only a single, compact radio-emitting feature was detected at mas-scale resolution indicates that the jet is not oriented close to the plane of the sky at pc scales.

The 1.4-GHz radio power of the source calculated from the flux density detected in the FIRST survey ( $\sim 150 \text{ mJy}$ ) is  $P_{1.4\text{GHz}}^{\text{total}} = 9 \cdot 10^{25} \text{ W Hz}^{-1}$ . An and Baan (2012) studied the evolutionary sequence of symmetric extragalactic radio sources. On their radio power versus projected linear size diagram, J1030+5516 is among the large symmetric objects and the low-power FR II radio galaxies.

The projected linear size of the source is  $D \sim 115 \text{ kpc}$ . Assuming a constant expansion velocity and using the limit  $\beta \cos i = 0.29$  derived from the kpc-scale radio structure, the kinematic age of the source can be estimated as

$$t_{\text{kin}} = \frac{D_0}{2\beta c} = \frac{D}{2\beta c \sin i} = \frac{D}{2 \cdot 0.29c \cdot \tan i} = \frac{6.3 \cdot 10^5}{\tan i} \text{ yr} \quad (5)$$

where  $D_0$  is the full (deprojected) size of the radio source. Using the upper limit on the inclination

angle ( $73^\circ$ ), the lower limit on the age of the kpc-scale radio structure is  $2 \cdot 10^5 \text{ yr}$ . The inclination angle of J1030+5516 should be below  $\sim 32^\circ$  to obtain an age  $\gtrsim 10^6 \text{ yr}$  and its age would reach  $10^7 \text{ yr}$ , if the inclination angle would be  $\lesssim 5^\circ$ , which is not consistent with a nearly symmetric kpc-scale structure. Thus, J1030+5516 seems to be younger than typical FRII radio galaxies whose lifetimes are estimated to be ( $10^6 - 10^7$ ) yr (O'Dea et al. 2009).

Rakshit et al. (2019) investigated the infrared properties of 520 NLS1 sources using *WISE* data. They found that more than 50% of the sources classified as variable in the AllWISE Source Catalog (Cutri et al. 2014) fall within a specific region in the *WISE* color-color diagram, the 'WISE Gamma-ray strip' (WGS). The WGS is defined by D'Abrusco et al. (2012) and Massaro et al. (2012) as a distinct region where blazars are located. The infrared colors of J1030+5516 place this source within the WGS as well. Based upon this and its radio-loudness, D'Abrusco et al. (2014) included J1030+5516 in the list of  $\gamma$ -ray emitting blazar candidates. They defined three classes of blazar candidate sources based on their decreasing likelihood of being blazars. J1030+5516 fell into the second class. This motivated us to analyse the available *Fermi*/LAT data to look for evidence of  $\gamma$ -ray emission. However, no  $\gamma$ -ray emission was found at the position of J1030+5516.

Rakshit et al. (2018) reported that J1030+5516 did not show variability in infrared at the wavelengths  $3.4\mu\text{m}$  and  $4.6\mu\text{m}$  measured with the *WISE* satellite. Since their publication, data from two additional epochs of *WISE* measurements became public. Our analysis of ten mission phases of the *WISE* data indicate a slight hint of long-term variability at the shorter wavelength due to the two additional epochs. There is no sign of short time scale (few day long) flux density changes neither in W1 nor in W2 bands.

Contrary to the finding of Rakshit et al. (2018), Graham et al. (2015) detected optical variability in J1030+5516. Graham et al. (2015) studied the optical light curves measured by the Catalina Real-time Transient Survey (Drake et al. 2009) to look for periodic variability in quasars, which they interpreted as induced by a closely separated binary supermassive black hole in those sources. They list J1030+5516 among the binary candidates with a period of 1515 days, a separation of 0.006 pc and a rest-frame merger time of  $2.2 \cdot 10^5 \text{ yr}$  (assuming a mass ratio of 0.5). However, Vaughan et al. (2016) called for cautious approach when only a few cycles are used to assess periodic variability. In any case, whether periodic or not, J1030+5516 seems to show some variability in optical and infrared bands on time scales of years, as suggested by Graham et al.

(2015) and perhaps also by our light curve compiled from *WISE* data (Fig. 2).

## 5 Summary and conclusion

To reveal its structural properties at high resolution, we analysed archival radio interferometric observations of J1030+5516, a recently discovered rare radio-loud NLS1 source (Rakshit et al. 2018) having kpc-scale extended structure reminiscent of FR II radio galaxies. The compact central core and the nearly symmetric hotspots on its two sides seen in our 5-GHz VLA A-configuration image (Fig. 1) are consistent with the lower-resolution 1.4-GHz VLA FIRST survey image. A large fraction, more than a half of the radio emission originates from diffuse structures related to the two lobes, and is resolved out with the VLA at 5 GHz. At even higher, mas-scale resolution, the 4.6 and 7.6 GHz VLBA observations show a single, unresolved core feature, with a brightness temperature  $T_B > 3 \cdot 10^9$  K. The observed high-resolution radio morphology and the derived parameters of J1030+5516 make it similar to the few known NLS1 sources with large-scale extended radio emission (Richards and Lister 2015; Gabányi et al. 2018b).

Using the arm-length ratio, we derived a lower limit for the kpc-scale jet speed ( $\beta > 0.3$ ), and a corresponding upper limit of the inclination angle,  $i < 73^\circ$ , which are slightly more stringent than the ones given by Rakshit et al. (2018). The lack of complex radio morphology at mas scale indicates that the inner jet of J1030+5516 is not oriented close to the plane of the sky at pc scales.

The *WISE* infrared colors of the source place it in the WGS. However, our analysis of all available *Fermi*/LAT data did not reveal any  $\gamma$ -ray emission at the position of J1030+5516. There is indication of at least some variability on a multi-year time scale, both in the mid-infrared based on the most complete *WISE* light curve (Fig. 2), and in the optical according to monitoring observations analysed by Graham et al. (2015). Based on two epochs of radio observations, we also found indication of flux density variability.

Our results support the conclusion of Rakshit et al. (2018) that the NLS1 galaxy J1030+5516 is likely a low-power and young version of an FR II radio galaxy with a double-lobed structure. There is no indication of relativistic boosting in J1030+5516, neither from radio imaging, nor from variability or  $\gamma$ -ray data, however it cannot be completely ruled out either.

## Acknowledgements

This project received support from the Hungarian Research, Development and Innovation Office (OTKA NN110333). K.É.G. was supported by the János Bolyai Research Scholarship of the Hungarian Academy of Sciences. P.V. acknowledges support from *Fermi* grant NNM11AA01A. We used in our work VLBA data from project BP192F7 provided by the National Radio Astronomy Observatory that is a facility of the National Science Foundation operated under cooperative agreement by Associated Universities, Inc. We thank Leonid Petrov for providing results of data analysis prior to publication. This publication makes use of data products from the Wide-field Infrared Survey Explorer, which is a joint project of the University of California, Los Angeles, and the Jet Propulsion Laboratory/California Institute of Technology, funded by the National Aeronautics and Space Administration.

Conflict of Interest: The authors declare that they have no conflict of interest.

## References

- Acero, F., Ackermann, M., Ajello, M., Albert, A., Atwood, W.B., Axelsson, M., Baldini, L., Ballet, J., Barbiellini, G., Bastieri, D., Belfiore, A., Bellazzini, R., Bissaldi, E., Blandford, R.D., Bloom, E.D., Bogart, J.R., Bonino, R., Bottacini, E., Bregeon, J., Britto, R.J., Bruel, P., Buehler, R., Burnett, T.H., Buson, S., Caliandro, G.A., Cameron, R.A., Caputo, R., Caragiulo, M., Caraveo, P.A., Casandjian, J.M., Cavazzuti, E., Charles, E., Chaves, R.C.G., Chekhtman, A., Cheung, C.C., Chiang, J., Chiaro, G., Ciprini, S., Claus, R., Cohen-Tanugi, J., Cominsky, L.R., Conrad, J., Cutini, S., D'Ammando, F., de Angelis, A., DeKlotz, M., de Palma, F., Desiante, R., Digel, S.W., Di Venere, L., Drell, P.S., Dubois, R., Dumora, D., Favuzzi, C., Fegan, S.J., Ferrara, E.C., Finke, J., Franckowiak, A., Fukazawa, Y., Funk, S., Fusco, P., Gargano, F., Gasparrini, D., Giebels, B., Giglietto, N., Giommi, P., Giordano, F., Giroletti, M., Glanzman, T., Godfrey, G., Grenier, I.A., Grondin, M.-H., Grove, J.E., Guillemot, L., Guiriec, S., Hadasch, D., Harding, A.K., Hays, E., Hewitt, J.W., Hill, A.B., Horan, D., Iafate, G., Jogler, T., Jóhannesson, G., Johnson, R.P., Johnson, A.S., Johnson, T.J., Johnson, W.N., Kamae, T., Kataoka, J., Katsuta, J., Kuss, M., La Mura, G., Landriau, D., Larsson, S., Latronico, L., Lemoine-Goumard, M., Li, J., Li, L., Longo, F., Loparco, F., Lott, B., Lovellette, M.N., Lubrano, P., Madejski, G.M., Massaro, F., Mayer, M., Mazziotta, M.N., McEnery, J.E., Michelson, P.F., Mirabal, N., Mizuno, T., Moiseev, A.A., Mongelli, M., Monzani, M.E., Morselli, A., Moskalenko, I.V., Murgia, S., Nuss, E., Ohno, M., Ohsugi, T., Omodei, N., Orienti, M., Orlando, E., Ormes, J.F., Paneque, D., Panetta, J.H., Perkins, J.S., Pesce-Rollins, M., Piron, F., Pivato, G., Porter, T.A., Racusin, J.L., Rando, R., Razzano, M., Razzaque, S., Reimer, A., Reimer, O., Reposeur, T., Rochester, L.S., Romani, R.W., Salvetti, D., Sánchez-Conde, M., Saz Parkinson, P.M., Schulz, A., Siskind, E.J., Smith, D.A., Spada, F., Spandre, G., Spinelli, P., Stephens, T.E., Strong, A.W., Suson, D.J., Takahashi, H., Takahashi, T., Tanaka, Y., Thayer, J.G., Thayer, J.B., Thompson, D.J., Tibaldo, L., Tibolla, O., Torres, D.F., Torresi, E., Tosti, G., Troja, E., Van Klavveren, B., Vianello, G., Winer, B.L., Wood, K.S., Wood, M., Zimmer, S., Fermi-LAT Collaboration: *Astrophys. J. Suppl. Ser.* **218**, 23 (2015). 1501.02003
- An, T., Baan, W.A.: *Astrophys. J.* **760**, 77 (2012). 1211.1760. doi:10.1088/0004-637X/760/1/77
- Becker, R.H., White, R.L., Helfand, D.J.: *Astrophys. J.* **450**, 559 (1995). doi:10.1086/176166
- Berton, M., Congiu, E., Järvelä, E., Antonucci, R., Kharb, P., Lister, M.L., Tarchi, A., Caccianiga, A., Chen, S., Foschini, L., Lähteenmäki, A., Richards, J.L., Ciroui, S., Cracco, V., Frezzato, M., La Mura, G., Rafanelli, P.: *Astron. Astrophys.* **614**, 87 (2018). 1801.03519. doi:10.1051/0004-6361/201832612
- Boroson, T.A., Green, R.F.: *Astrophys. J. Suppl. Ser.* **80**, 109 (1992). doi:10.1086/191661
- Congiu, E., Berton, M., Giroletti, M., Antonucci, R., Caccianiga, A., Kharb, P., Lister, M.L., Foschini, L., Ciroui, S., Cracco, V., Frezzato, M., Järvelä, E., La Mura, G., Richards, J.L., Rafanelli, P.: *Astron. Astrophys.* **603**, 32 (2017). 1704.03881
- Cracco, V., Ciroui, S., Berton, M., Di Mille, F., Foschini, L., La Mura, G., Rafanelli, P.: *Mon. Not. R. Astron. Soc.* **462**, 1256 (2016). 1607.03438
- Cutri, R.M., et al.: *VizieR Online Data Catalog*, 328 (2014)
- D'Abrusco, R., Massaro, F., Ajello, M., Grindlay, J.E., Smith, H.A., Tosti, G.: *Astrophys. J.* **748**, 68 (2012). 1203.0568
- D'Abrusco, R., Massaro, F., Paggi, A., Smith, H.A., Masetti, N., Landoni, M., Tosti, G.: *Astrophys. J. Suppl. Ser.* **215**, 14 (2014). 1410.0029
- Decarli, R., Dotti, M., Fontana, M., Haardt, F.: *Mon. Not. R. Astron. Soc.* **386**, 15 (2008). 0801.4560. doi:10.1111/j.1745-3933.2008.00451.x
- Doi, A., Nagira, H., Kawakatu, N., Kino, M., Nagai, H., Asada, K.: *Astrophys. J.* **760**, 41 (2012). 1210.1303
- Douglas, J.N., Bash, F.N., Bozayan, F.A., Torrence, G.W., Wolfe, C.: *Astron. J.* **111**, 1945 (1996). doi:10.1086/117932
- Drake, A.J., Djorgovski, S.G., Mahabal, A., Beshore, E., Larson, S., Graham, M.J., Williams, R., Christensen, E., Catelan, M., Boattini, A., Gibbs, A., Hill, R., Kowalski, R.: *Astrophys. J.* **696**, 870 (2009). 0809.1394
- Fanaroff, B.L., Riley, J.M.: *Mon. Not. R. Astron. Soc.* **167**, 31 (1974)
- Gabányi, K., Moór, A., Frey, S.: In: *Revisiting narrow-line Seyfert 1 galaxies and their place in the Universe. Proceedings of Science, PoS(NLS1-2018)042* (2018a). 1807.05802
- Gabányi, K., Frey, S., Paragi, Z., Järvelä, E., Morokuma, T., An, T., Tanaka, M., Tar, I.: *Mon. Not. R. Astron. Soc.* **473**, 1554 (2018b). 1709.07202
- Giovannini, G., Cotton, W.D., Feretti, L., Lara, L., Venturi, T.: *Astrophys. J.* **552**, 508 (2001). astro-ph/0101096. doi:10.1086/320581
- Goodrich, R.W.: *Astrophys. J.* **342**, 224 (1989)
- Graham, M.J., Djorgovski, S.G., Stern, D., Drake, A.J., Mahabal, A.A., Donalek, C., Glikman, E., Larson, S., Christensen, E.: *Mon. Not. R. Astron. Soc.* **453**, 1562 (2015). 1507.07603
- Greisen, E.W.: In: Heck, A. (ed.) *Information Handling in Astronomy - Historical Vistas. Astrophysics and Space Science Library*, vol. 285, p. 109 (2003)
- Gu, M., Chen, Y., Komossa, S., Yuan, W., Shen, Z., Wajima, K., Zhou, H., Zensus, J.A.: *The Astrophysical Journal Supplement Series* **221**, 3 (2015). 1509.01889
- Kellermann, K.I., Sramek, R., Schmidt, M., Shaffer, D.B., Green, R.: *Astron. J.* **98**, 1195 (1989)
- Komossa, S., Voges, W., Xu, D., Mathur, S., Adorf, H.-M., Lemson, G., Duschl, W.J., Grupe, D.: *Astron. J.* **132**, 531 (2006). astro-ph/0603680
- Kovalev, Y.Y., Kellermann, K.I., Lister, M.L., Homan, D.C., Vermeulen, R.C., Cohen, M.H., Ros, E., Kadler, M., Lobanov, A.P., Zensus, J.A., Kardashev, N.S., Gurvits, L.I., Aller, M.F., Aller, H.D.: *Astron. J.* **130**, 2473 (2005). astro-ph/0505536
- Lister, M.L., Aller, M.F., Aller, H.D., Homan, D.C., Kellermann, K.I., Kovalev, Y.Y., Pushkarev, A.B., Richards, J.L., Ros, E., Savolainen, T.: *Astron. J.* **152**, 12 (2016). 1603.03882

- Longair, M.S., Riley, J.M.: *Mon. Not. R. Astron. Soc.* **188**, 625 (1979)
- Mainzer, A., Bauer, J., Cutri, R.M., Grav, T., Masiero, J., Beck, R., Clarkson, P., Conrow, T., Dailey, J., Eisenhardt, P., Fabinsky, B., Fajardo-Acosta, S., Fowler, J., Gelino, C., Grillmair, C., Heinrichsen, I., Kendall, M., Kirkpatrick, J.D., Liu, F., Masci, F., McCallon, H., Nugent, C.R., Papin, M., Rice, E., Royer, D., Ryan, T., Sevilla, P., Sonnett, S., Stevenson, R., Thompson, D.B., Wheelock, S., Wiemer, D., Wittman, M., Wright, E., Yan, L.: *Astrophys. J.* **792**, 30 (2014). 1406.6025
- Massaro, F., D'Abrusco, R., Tosti, G., Ajello, M., Gasparini, D., Grindlay, J.E., Smith, H.A.: *Astrophys. J.* **750**, 138 (2012). 1203.1330
- Mathur, S.: *Mon. Not. R. Astron. Soc.* **314**, 17 (2000). [astro-ph/0003111](#)
- O'Dea, C.P., Daly, R.A., Kharb, P., Freeman, K.A., Baum, S.A.: *Astron. Astrophys.* **494**, 471 (2009). 0810.1213. doi:10.1051/0004-6361:200809416
- Osterbrock, D.E., Pogge, R.W.: *Astrophys. J.* **297**, 166 (1985)
- Rakshit, S., Stalin, C.S., Hota, A., Konar, C.: *Astrophys. J.* **869**, 173 (2018). 1811.02147. doi:10.3847/1538-4357/aafe8
- Rakshit, S., Johnson, A., Stalin, C.S., Gandhi, P., Hoenig, S.: *Mon. Not. R. Astron. Soc.* **483**, 2362 (2019). 1811.11372. doi:10.1093/mnras/sty3261
- Readhead, A.C.S.: *Astrophys. J.* **426**, 51 (1994)
- Romano, P., Vercellone, S., Foschini, L., Tavecchio, F., Landoni, M., Knödseder, J.: *Mon. Not. R. Astron. Soc.* **481**, 5046 (2018). 1809.03426. doi:10.1093/mnras/sty2484
- Richards, J.L., Lister, M.L.: *Astrophys. J.* **800**, 8 (2015). 1501.05299
- Shepherd, M.C., Pearson, T.J., Taylor, G.B.: *Bull. Am. Astron. Soc.* **26**, 987 (1994)
- Singh, V., Chand, H.: *Mon. Not. R. Astron. Soc.* **480**, 1796 (2018). 1807.01945
- Taylor, G.B., Vermeulen, R.C.: *Astrophys. J. Lett.* **485**, 9 (1997). [astro-ph/9706011](#)
- Vaughan, S., Uttley, P., Markowitz, A.G., Huppenkothen, D., Middleton, M.J., Alston, W.N., Scargle, J.D., Farr, W.M.: *Mon. Not. R. Astron. Soc.* **461**, 3145 (2016). 1606.02620
- Wood, M., Caputo, R., Charles, E., Di Mauro, M., Magill, J., Perkins, J.S., Fermi-LAT Collaboration: In: 35th International Cosmic Ray Conference, Proceedings of Science, PoS(ICRC2017)824 (2017). 1707.09551
- Wright, E.L., Eisenhardt, P.R.M., Mainzer, A.K., Ressler, M.E., Cutri, R.M., Jarrett, T., Kirkpatrick, J.D., Padgett, D., McMillan, R.S., Skrutskie, M., Stanford, S.A., Cohen, M., Walker, R.G., Mather, J.C., Leisawitz, D., Gautier, T.N. III, McLean, I., Benford, D., Lonsdale, C.J., Blain, A., Mendez, B., Irace, W.R., Duval, V., Liu, F., Royer, D., Heinrichsen, I., Howard, J., Shannon, M., Kendall, M., Walsh, A.L., Larsen, M., Cardon, J.G., Schick, S., Schwalm, M., Abid, M., Fabinsky, B., Naes, L., Tsai, C.-W.: *Astron. J.* **140**, 1868 (2010). 1008.0031
- Yuan, W., Zhou, H.Y., Komossa, S., Dong, X.B., Wang, T.G., Lu, H.L., Bai, J.M.: *Astrophys. J.* **685**, 801 (2008). 0806.3755
- Zhou, H., Wang, T., Yuan, W., Lu, H., Dong, X., Wang, J., Lu, Y.: *Astrophys. J. Suppl. Ser.* **166**, 128 (2006). [astro-ph/0603759](#)